

Synthesis and Characterization of Nickel Ferrite Nanoparticles via the Ultrasonic-Assisted Sonochemical Method

Atul P. Keche**^a

^aDepartment of Physics

R. B. Attal Arts, Science & Commerce College, Georai, Beed, India

Corresponding author: meetatulkeche@gmail.com

Abstract: Nickel ferrite (NiFe_2O_4) nanoparticles, a significant class of soft ferrimagnetic materials, are widely explored for their unique physicochemical and magnetic properties. This paper provides a comprehensive review of the synthesis, characterization, and applications of these nanoparticles, with a focus on the ultrasonic-assisted sonochemical method. This "green" and energy-efficient technique leverages acoustic cavitation, which creates localized "hot spots" with extreme temperatures and pressures, enabling the rapid formation of highly crystalline nanoparticles. The article details how synthesis parameters like sonication time, power, and pH can be precisely controlled to tailor the material's properties. Various characterization techniques, including X-ray diffraction, electron microscopy, and vibrating sample magnetometry, are discussed to elucidate the crystal structure, morphology, and magnetic behavior, from ferrimagnetic to superparamagnetic. The review concludes by highlighting the diverse applications of these tunable nanoparticles, such as in environmental remediation, high-frequency electronics, and advanced biomedical applications like MRI and magnetic particle imaging

Keywords: Nickel Ferrite, Nanoparticles, Sonochemical, Acoustic, Characterization

I. INTRODUCTION

Spinel ferrites represent a significant class of metal oxides with the general chemical formula AB_2O_4 , where A and B are metal cations. These materials are characterized by a cubic close-packed (fcc) arrangement of oxygen anions, with cations occupying specific tetrahedral (A) and octahedral (B) interstitial sites [1]. The versatility of spinel ferrites is immense, as the substitution of different divalent metal cations at the M-site (nickel, cobalt, magnesium, or zinc) allows for the precise tuning of their physicochemical and functional properties [2]. As a result, these materials are widely used in various applications, ranging from high-frequency electronics to biomedical fields, due to their interesting and important properties, such as low melting points, high specific heating, and favorable electrical and magnetic traits. While their use dates back to the naturally occurring magnetic mineral magnetite (Fe_3O_4), the full potential and systematic study of these materials were not realized until the emergence of nanotechnology in the 1990s [3].

Properties and Structure of Nickel Ferrite (NiFe_2O_4)

Among the diverse family of spinel ferrites, nickel ferrite (NiFe_2O_4) is a particularly important and well-studied material. It is classified as a soft ferrimagnetic material, which means it can be easily magnetized and demagnetized, making it suitable for a wide range of applications. The remarkable properties of NiFe_2O_4 stem from its unique crystal structure. It is a completely inverse spinel, which is represented by the formula $(\text{Fe}^{3+})_A[\text{Ni}^{2+}\text{Fe}^{3+}]_B\text{O}_4$ [4, 5]. In this configuration, all the divalent nickel ions (Ni^{2+}) are located exclusively at the octahedral B-sites, while the trivalent iron ions (Fe^{3+}) are distributed equally between the tetrahedral A-sites and the octahedral B-sites. This specific cation distribution and occupancy directly influence its magnetic and electrical properties, making it a subject of extensive research [6, 7].



Brief Review of Conventional Synthesis Methods and Their Limitations

The synthesis of high-quality NiFe_2O_4 nanoparticles with controlled size, shape, and crystallinity is a critical prerequisite for their effective application. Conventional synthesis techniques include the solid-state reaction, which typically requires extremely high temperatures ($+950^\circ\text{C}$), resulting in large particle sizes and potential inhomogeneity [8, 9]. Other established chemical methods include co-precipitation, sol-gel, hydrothermal synthesis, and combustion synthesis. However, these traditional approaches often face limitations such as long processing times, high energy consumption, and the use of hazardous chemicals, which can compromise the quality of the final product and its environmental footprint. For example, the conventional double sintering technique requires heating to at least 1573 K to achieve the formation of homogeneous grains. These drawbacks have motivated the search for more efficient, economical, and environmentally friendly synthesis routes [10].

Rationale for Sonochemical Synthesis: Advantages and Principles

The ultrasonic-assisted sonochemical method has emerged as a powerful, green, and cost-effective alternative for the synthesis of nanoparticles. This technique offers numerous advantages over conventional methods, including accelerated reaction rates, improved product purity, and a narrower size distribution of nanoparticles. The use of ultrasound can significantly reduce the size of the final particles and prevent their agglomeration, leading to a more uniform and highly crystalline product [11]. Furthermore, it allows for the synthesis of crystalline phases at much lower temperatures compared to high-temperature solid-state reactions. An important characteristic of this method is that while sonication alone may not always be sufficient to produce the final crystalline spinel structure in a single step, its effects are highly beneficial for subsequent processing [12]. For instance, some sonochemical procedures yield intermediate amorphous hydroxides or oxides, which then require a final, lower-temperature calcination step to form the desired crystalline spinel structure. The primary role of sonication in such a process is to create a highly dispersed, reactive precursor material. This pre-treatment step fundamentally changes the material's properties, making it more reactive in the subsequent thermal process. This is evident in studies where sonochemically prepared samples form homogeneous grains at a much lower sintering temperature (1373 K) compared to conventionally prepared samples (1573 K). This ability to accelerate and facilitate the reaction at lower energy inputs makes the sonochemical approach a valuable technique for the synthesis of advanced nanomaterials [13].

II. PRINCIPLES OF ULTRASONIC-ASSISTED SONOCHEMICAL SYNTHESIS

The Phenomenon of Acoustic Cavitation

The foundation of sonochemistry lies in a unique physical phenomenon known as acoustic cavitation. This process is initiated by the application of high-intensity ultrasonic waves to a liquid medium, which causes a rapid succession of high-pressure (compression) and low-pressure (rarefaction) cycles [14]. During the low-pressure cycle, the liquid's tensile strength is overcome, leading to the formation of small, oscillating gas bubbles. These bubbles continue to grow with each successive cycle of applied ultrasonic energy until they reach an unstable size, at which point they undergo a violent and rapid implosive collapse. This implosion is the central event responsible for the unique chemical and physical effects of sonochemistry [15].

The "Hot Spot" Theory: Creation of Extreme Localized Conditions

The implosive collapse of the cavitation bubbles is so rapid that the heat generated by the compression of the gas inside the bubble cannot dissipate into the surrounding liquid (an adiabatic process). This leads to the creation of a transient, localized "hot spot" within the micro-reactor of the collapsing bubble [16]. These extreme conditions within the hot spot are what drive high-energy chemical reactions in an otherwise cold liquid. Research has estimated the temperatures within these hot spots to be as high as 5,000 K, with pressures reaching approximately 1,000 atm. This event is also characterized by extraordinarily rapid heating and cooling rates, on the order of 10^{10} K s^{-1} . The "hot spot" theory is the widely accepted explanation for the origin of both sonochemistry and sonoluminescence, a phenomenon where light is emitted during the collapse [17, 18].

Physical and Chemical Effects of Ultrasound in Nanomaterial Synthesis

The effects of ultrasonic waves in a liquid medium are twofold: physical and chemical. The physical effects, which are particularly relevant for multiphase systems (e.g., liquid-solid suspensions), include the formation of high-speed microjets and powerful shock waves. These phenomena arise from the asymmetrical collapse of bubbles near a solid surface. Such effects are highly effective at surface cleaning and erosion, which leads to improved mass transport and the prevention of particle agglomeration [19]. The chemical effects are a direct consequence of the extreme conditions within the "hot spots." The high temperatures and pressures can induce the thermal dissociation of solvent molecules, such as water, into highly reactive free radicals. A prime example is the sonolysis of water: These radicals can then participate in a variety of chemical reactions, leading to novel reaction pathways that would not occur under normal conditions. The delicate interplay between these physical and chemical effects is what gives the sonochemical method its power in nanoparticle synthesis [20].

Mechanism of Nucleation and Growth under Sonochemical Conditions

The extreme conditions created by acoustic cavitation provide a unique environment for the nucleation and growth of nanoparticles. The highly reactive species and rapid temperature fluctuations can facilitate chemical reactions, such as the formation of metal hydroxides or oxides from precursor salts. The shock waves and high-velocity liquid jets generated by cavitation can also cause high-speed inter-particle collisions, which change particle morphology and surface properties. The efficacy of sonochemistry in nanomaterial synthesis is rooted in a balance between its physical and chemical effects [21]. The physical phenomena, such as enhanced mass transport and de-agglomeration, are essential for creating a homogeneous reaction environment, which ensures a uniform final product. Simultaneously, the chemical effects, specifically the generation of radicals and high-energy conditions, provide the necessary activation energy for the chemical transformation. This explains why the method can produce highly reactive precursor particles that are already partially formed and dispersed, thus reducing the energy barrier for subsequent thermal processing. This synergy allows for the production of materials with superior properties that are difficult to achieve with either conventional chemical synthesis or high-temperature bulk methods alone [22, 23].

III. SYNTHESIS OF NICKEL FERRITE NANOPARTICLES VIA THE SONOCHEMICAL METHOD

Selection of Precursors and Reaction Media

The choice of precursor materials is a critical step in the sonochemical synthesis of NiFe_2O_4 nanoparticles. One approach, which requires volatile precursors, involves the use of toxic and hazardous organic compounds such as iron pentacarbonyl ($\text{Fe}(\text{CO})_5$) and nickel tetracarbonyl ($\text{Ni}(\text{CO})_4$) dissolved in a decalin solution. This method is effective because the reaction primarily occurs in the vapor phase within the cavitation bubbles.

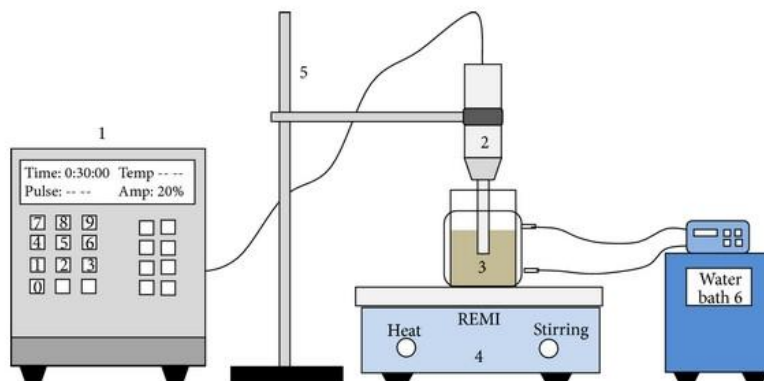


Figure 1 Ultrasonochemical synthesis of NiFe_2O_4 nanoparticles

However, due to the high toxicity of these precursors, a more common and "greener" approach utilizes metal nitrates or chlorides. Typical precursors include nickel nitrate hexahydrate ($\text{Ni}(\text{NO}_3)_2 \cdot 6\text{H}_2\text{O}$) and iron nitrate nonahydrate ($\text{Fe}(\text{NO}_3)_3 \cdot 9\text{H}_2\text{O}$).

$)_3 \cdot 9H_2O$), which are dissolved in deionized water, typically with a stoichiometric molar ratio of nickel to iron of 1:2 to achieve the desired $NiFe_2O_4$ stoichiometry. Additionally, a stabilizing agent such as polyethylene glycol (PEG) is often added to the solution to aid in particle dispersion and prevent agglomeration.

IV. EXPERIMENTAL PROCEDURE

A typical sonochemical synthesis procedure for $NiFe_2O_4$ nanoparticles involves a series of controlled steps. First, the metal precursors ($Ni(NO_3)_2 \cdot 6H_2O$ and $Fe(NO_3)_3 \cdot 9H_2O$) are accurately weighed and dissolved in a suitable solvent, such as deionized water. A base, such as sodium hydroxide (NaOH), is then added dropwise to the mixture while stirring to adjust the pH to an alkaline value, typically in the range of 11-13, which facilitates the precipitation of metal hydroxides. The prepared solution is then subjected to ultrasonic irradiation using a high-intensity ultrasonic probe or bath. A typical probe might operate at a frequency of 20 kHz with an intensity of 100 W/cm². After a specified sonication time, a black or brown-colored precipitate is obtained. This precipitate is then separated from the solution, washed repeatedly to remove impurities, and dried, often in a vacuum oven. The as-synthesized material is often in an amorphous or semi-crystalline state and may contain unreacted oxide phases. Therefore, a subsequent heat treatment or calcination step is often performed to achieve the final, fully crystalline inverse spinel structure. This calcination is typically carried out at temperatures ranging from 573 K to 773 K.



Influence of Synthesis Parameters on Nanoparticle Properties

Effect of Sonication Time and Power

The sonication time and power are critical parameters that directly influence the final properties of the nanoparticles. Studies have demonstrated that increasing both sonication time and power leads to a decrease in the average particle size and helps prevent agglomeration, resulting in a more uniform particle dispersion. Prolonged sonication can also be effective in reducing or eliminating amorphous and secondary phases, leading to higher purity and crystallinity in the final product.

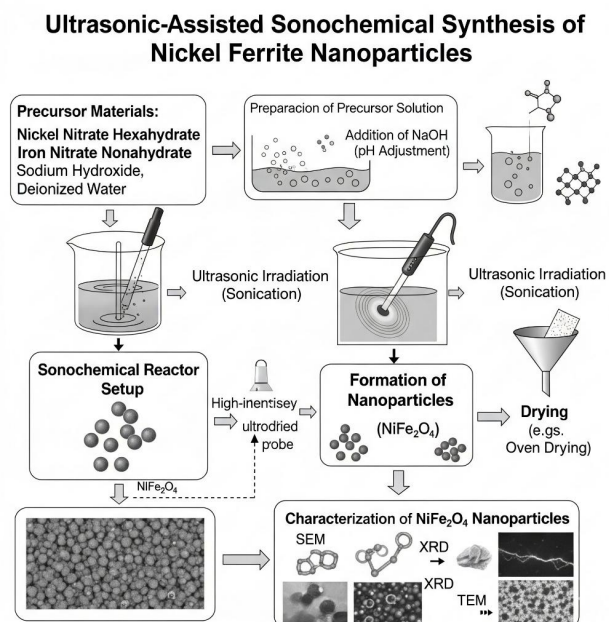


Figure 2 Experimental procedure for the ultrasonic-assisted sonochemical synthesis of nickel ferrite nanoparticles

However, the relationship is not without its complexities. While sonication is essential for de-agglomeration, there is a limit to its beneficial effects. Extended sonication can cause particle fragmentation and even lead to the dissolution of the nanoparticles, which can alter their surface chemistry. For biomedical applications, this phenomenon is particularly important, as it could result in the release of toxic metal ions, compromising the material's biocompatibility. Therefore, optimizing the sonication parameters is crucial to achieve the desired particle characteristics without inducing adverse effects.

Role of pH and Precursor Concentration

The pH of the reaction solution is a fundamental parameter that governs the synthesis process. A high pH, typically maintained between 11 and 13, is necessary to ensure the complete precipitation of the metal precursors as hydroxides. The pH also plays a crucial role in determining the final surface charge of the nanoparticles, which has significant implications for their applications. The point of zero charge (pHPZC) for sonochemically prepared NiFe₂O₄ nanoparticles has been determined to be approximately 6. At a pH greater than this value, the surface of the nanoparticles becomes negatively charged, making them suitable for the adsorption of cationic species, such as Methylene Blue dye. Conversely, at a pH below 6, the surface is positively charged. This direct link between a controllable synthesis parameter (pH) and a fundamental material property (surface charge) illustrates the fine-tuning capability of the sonochemical method [24, 25].

Impact of Post-Synthesis Calcination Temperature

The post-synthesis calcination temperature is a key factor that influences the final properties of the NiFe₂O₄ nanoparticles. An increase in calcination temperature leads to an increase in both particle size and crystallinity. The sonochemical method is particularly advantageous in this regard, as it allows for the formation of homogeneous, crystalline grains at a significantly lower sintering temperature (1373 K) compared to the conventional method (1573 K). This is because the sonochemical process creates a highly reactive and well-dispersed precursor, reducing the energy required for the final phase transformation [26]. The thermal treatment also affects the lattice structure. As the calcination temperature increases, the residual strain within the nanoparticles decreases, which is a key indicator of improved crystallinity and a reduction in lattice defects. This highlights that thermal energy is necessary to overcome the activation energy barrier for the transformation of the amorphous precursors into the ordered spinel phase. The sonochemical step effectively lowers this barrier, allowing for the formation of a superior material with less energy input [27].

V. CHARACTERIZATION OF SONOCHEMICALLY SYNTHESIZED NIFE₂O₄

To confirm the successful synthesis and to understand the properties of the prepared NiFe₂O₄ nanoparticles, a suite of advanced characterization techniques is employed.

Structural Analysis: X-ray Diffraction (XRD)

X-ray Diffraction (XRD) is the primary method for determining the crystal structure, phase purity, and crystallite size of the synthesized nanoparticles. The XRD pattern of successfully synthesized NiFe₂O₄ nanoparticles will exhibit a single-phase cubic spinel structure with a face-centered cubic (fcc) lattice and the Fd $\bar{3}$ m space group. The broadness of the diffraction peaks is a characteristic feature of nanomaterials, with broader peaks indicating a smaller crystallite size. Crystallite size can be quantitatively calculated using the Debye-Scherrer formula, while the Williamson-Hall equation is utilized to assess the contributions of crystallite size and lattice strain to the peak broadening [28, 29].

Morphological and Size Analysis: Transmission/Scanning Electron Microscopy (TEM/SEM)

Electron microscopy techniques, such as Scanning Electron Microscopy (SEM) and Transmission Electron Microscopy (TEM), are indispensable for visualizing the morphology, size, and degree of agglomeration of the nanoparticles. Sonochemically prepared NiFe₂O₄ nanoparticles are typically spherical and ultrafine, with reported average sizes often less than 5 nm in their as-synthesized state. High-Resolution TEM (HRTEM) images are capable of revealing the presence of lattice fringes, which provides direct visual evidence of the material's crystalline nature even without a

post-synthesis calcination step. Additionally, the Selected Area Electron Diffraction (SAED) pattern, which consists of concentric rings, provides further confirmation of the polycrystalline nature of the sample [30, 31].

Spectroscopic and Chemical Analysis (FTIR, UV-Vis, XPS)

Spectroscopic methods provide further details on the chemical and electronic properties of the nanoparticles. Fourier-Transform Infrared (FTIR) spectroscopy is used to identify the characteristic absorption bands corresponding to the metal-oxygen bonds in the tetrahedral (A) and octahedral (B) sites, typically observed near 600 cm^{-1} and 490 cm^{-1} respectively. UV-Visible (UV-Vis) spectroscopy is employed to investigate the optical properties of the material and determine its energy band gap. The energy band gap can be calculated from the absorption data using Tauc plots. A direct correlation exists between the synthesis parameters and the optical properties of the nanoparticles. For instance, the red-shift of absorption bands with increasing calcination temperature is a direct result of the increase in particle size, a phenomenon related to the quantum size effect. This demonstrates how synthesis control can be used to tune a material's fundamental optical properties. X-ray Photoelectron Spectroscopy (XPS) is a powerful technique for confirming the elemental composition and oxidation states of the cations. XPS analysis on NiFe_2O_4 nanoparticles confirms the presence of Ni^{2+} and Fe^{3+} oxidation states, validating the successful formation of the target composition and its high redox activity [32, 33].

Table 1: Comparison of Characterization Techniques for NiFe_2O_4 Nanoparticles

Technique	Purpose	Key Information Provided
X-ray Diffraction (XRD)	Structural analysis, phase purity	Crystal structure, phase identification, crystallinity, crystallite size, lattice strain
Transmission/Scanning Electron Microscopy (TEM/SEM)	Morphological and size analysis	Particle shape, size, morphology, agglomeration, crystallinity (HRTEM)
Vibrating Sample Magnetometer (VSM)	Magnetic properties analysis	Saturation magnetization (Ms), coercivity (Hc), remanence (Mr), magnetic behavior (ferrimagnetic/superparamagnetic)
Fourier-Transform Infrared (FTIR)	Spectroscopic analysis	Presence of functional groups and characteristic metal-oxygen bonds in tetrahedral and octahedral sites
UV-Visible Spectroscopy	Optical properties analysis	Optical band gap, absorption characteristics
X-ray Photoelectron Spectroscopy (XPS)	Chemical state analysis	Elemental composition, oxidation states of cations ($\text{Ni}^{2+}, \text{Fe}^{3+}$)

VI. PHYSICOCHEMICAL AND MAGNETIC PROPERTIES

Crystal Structure and Cation Distribution

As discussed, the magnetic properties of nickel ferrite nanoparticles are intrinsically linked to their crystal structure and cation distribution. NiFe_2O_4 possesses a completely inverse spinel structure, with the formula $(\text{Fe}^{3+})_A[\text{Ni}^{2+}\text{Fe}^{3+}]_B\text{O}_4$. This distribution, where half of the Fe^{3+} ions occupy the tetrahedral A-sites and the remaining half, along with all the Ni^{2+} ions, occupy the octahedral B-sites, is of paramount importance. The physical properties of ferrites, including their remarkable electrical and magnetic traits, are directly dependent on the types of cations present and their distribution among these interstitial sites [34].

Origin of Ferrimagnetism: Neel's Theory and Superexchange Interactions

The magnetic behavior of spinel ferrites is characterized by ferrimagnetism, a phenomenon where the magnetic moments of cations in the tetrahedral (A) and octahedral (B) sublattices align anti-parallel to one another, resulting in a net magnetic moment. This ordering is governed by a series of superexchange interactions between the cations, which are mediated by the intervening oxygen anions. The A-O-B interaction is the strongest and is antiferromagnetic, dominating the magnetic properties [35]. The intrasublattice B-O-B interaction is ferromagnetic, while the A-O-A interaction is also antiferromagnetic but weaker than the A-B interaction. The temperature dependence of the magnetic

properties of NiFe₂O₄ can be effectively analyzed using the molecular field theory developed by Neel. According to this theory, the magnetic moments on the A and B sites oppose each other, and since the B-site contains twice as many cations as the A-site in a fully inverse spinel, the net magnetic moment is determined by the difference between the magnetic moments of the two sublattices [36].

Magnetic Properties of Nanoparticles

Nanosized NiFe₂O₄ exhibits distinct magnetic properties compared to its bulk, multi-domain counterpart, which are highly sensitive to particle size, shape, and purity.

Saturation Magnetization (Ms) and Coercivity (Hc)

The saturation magnetization (Ms) and coercivity (Hc) of NiFe₂O₄ nanoparticles are generally lower than their bulk values. The reported values for Ms can vary widely depending on the synthesis method and post-treatment, ranging from 39.60 emu/g for a hydrothermal method to 61.4 emu/g for a sol-gel technique. Both Ms and Hc have been shown to increase with increasing synthesis time, calcination temperature, and particle size. This is attributed to the increase in crystallinity and the enhancement of exchange interactions between the A and B sublattices as the particle size increases [37, 38].

Superparamagnetic Behavior

A key characteristic of nanosized NiFe₂O₄ is its superparamagnetic behavior at room temperature, which is observed when the particle size is below a critical diameter, typically around 30 nm. Superparamagnetism is a state where the particles behave like a single magnetic domain and their magnetic moments can spontaneously fluctuate, eliminating both coercivity and remanence in their hysteresis loops [39]. This property is highly desirable for biomedical applications, such as MRI and magnetic hyperthermia, as it allows for the manipulation of the nanoparticles using an external magnetic field without the risk of permanent magnetization and agglomeration [40].

Correlation between Synthesis Parameters and Final Properties

The synthesis method, especially the use of sonochemistry, directly dictates the particle's morphology and size, which in turn controls its magnetic properties. The ability of the sonochemical method to produce ultrafine particles (<5 nm) is directly responsible for the observed superparamagnetic behavior at room temperature [41]. A direct and clear cause-and-effect relationship exists: as the particle size increases (a consequence of longer sonication time, higher calcination temperature, etc.), the material transitions from a single-domain superparamagnetic state to a multi-domain ferrimagnetic state. This transition is marked by a noticeable increase in both Ms and Hc. This dependency of magnetic properties on synthesis parameters is a powerful illustration of how the sonochemical method allows for the fine-tuning of material properties for specific applications [42].

Table 2 Magnetic Properties of NiFe₂O₄ Nanoparticles

Synthesis Method	Particle Size (nm)	Saturation Magnetization (Ms) (emu/g)	Coercivity (Hc) (Oe)	Magnetic Behavior
Hydrothermal	29	3.25	2.5	Ferromagnetic
Hydrothermal (12h)	58	4.98	6.5	Ferromagnetic
Hydrothermal	50-60	39.60	15.67	Superparamagnetic
Sol-gel	~9.7	~61.4	-	Ferromagnetic (at 10 K)
Sol-gel	90	-	-	Ferromagnetic
Sonochemical	<5	-	-	Ferrimagnetic
Alcohol-solution combustion	-	-	0	Superparamagnetic

VII. APPLICATIONS OF SONOCHEMICALLY PREPARED NiFe₂O₄ NANOPARTICLES

The unique physicochemical and magnetic properties of NiFe₂O₄ nanoparticles, particularly those synthesized via the sonochemical method, make them highly suitable for a diverse range of applications.

Environmental Remediation: Catalysis and Wastewater Treatment

Spinel ferrites are recognized as highly efficient catalysts due to their high catalytic efficiency, ease of synthesis, and reusability, which is facilitated by their magnetic nature. Sonochemically synthesized NiFe₂O₄ has been successfully used in the degradation of organic pollutants, such as Chrysoidine R dye, in wastewater. The catalytic mechanism primarily involves the generation of highly reactive hydroxyl radicals ($\cdot\text{OH}$) and other oxidizing species from the dissociation of hydrogen peroxide (H₂O₂). The presence of NiFe₂O₄ enhances the formation of these radicals through a series of redox reactions involving the iron and nickel ions [43].



The sonochemical synthesis method itself improves the catalytic performance by producing nanoparticles with a smaller particle size and enhanced crystallinity, which in turn increases the material's surface area and the number of active catalytic sites. The magnetic nature of the catalyst also allows for its easy and efficient separation from the treated water using an external magnetic field, promoting its reuse and aligning with green chemistry principles [44].

Biomedical Applications

Magnetic nanoparticles, including NiFe₂O₄, have been at the forefront of biomedical research for decades, primarily for their use as contrast agents in Magnetic Resonance Imaging (MRI) and as tracer agents in Magnetic Particle Imaging (MPI). In MRI, these nanoparticles generate local magnetic field inhomogeneities that shorten the T₂ and T₂* relaxation times of surrounding water protons, resulting in a darker, hypointense signal in T₂- or T₂*-weighted images. In contrast, MPI is a non-invasive imaging modality that directly detects the magnetic nanoparticles. The technique relies on the non-linear magnetic response of superparamagnetic nanoparticles to an external oscillating magnetic field, which generates a measurable signal. This provides a highly specific signal of the nanoparticle distribution, which can then be co-localized with anatomical images from other modalities like MRI or CT. The ability to tailor the magnetic properties of NiFe₂O₄ nanoparticles, such as enhancing their signal in MPI by altering their composition, makes them highly promising for combined MRI/MPI imaging.

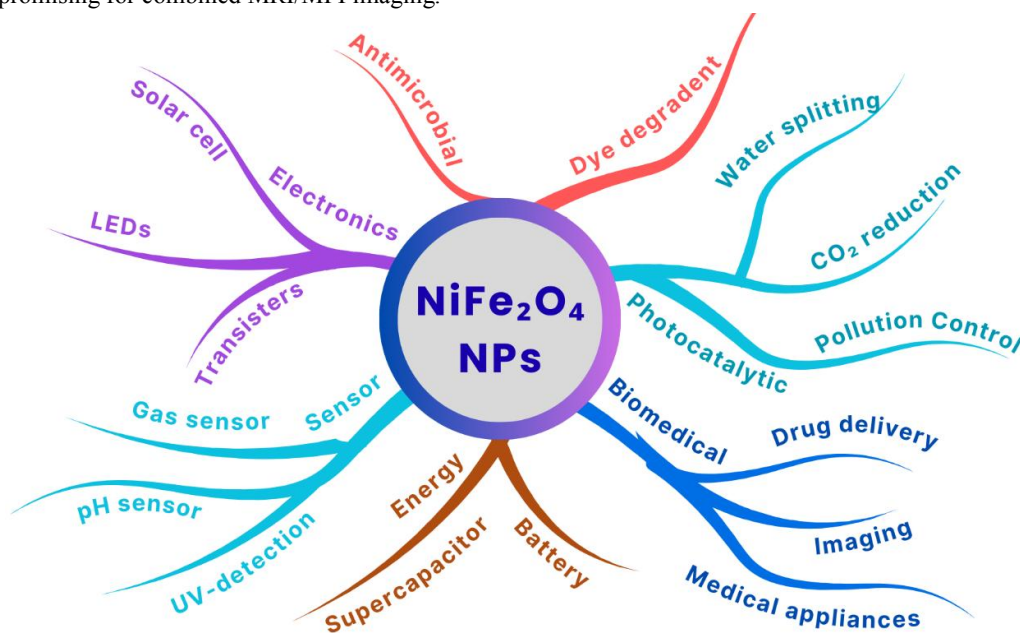


Figure 3 Applications of ultrasonic-assisted sonochemical synthesized nickel ferrite nanoparticles



High-Frequency Electronics and Sensors

NiFe_2O_4 is a valuable soft magnetic material for applications in high-frequency electronics due to its unique combination of low conductivity, high electrical resistivity, and high permeability. These properties are crucial for minimizing eddy current losses at high frequencies, making the material ideal for use in microwave absorbers and high-density magnetic recording devices. Sonochemically prepared NiFe_2O_4 nanoparticles have also been explored as a potential electrode material for supercapacitors, exhibiting a specific capacitance of over 600 F g^{-1} in one study, suggesting their utility for energy storage applications. The material's unique properties also lend themselves to sensor applications, such as the electrochemical detection of paracetamol [45, 46].

Emerging Applications in Energy Storage and Conversion

The field of energy research is a growing area for nickel ferrite nanoparticles. Beyond their use in supercapacitors, recent studies have explored their potential as photocatalysts and in thermoelectric materials. The development of novel nanocomposites, such as NiFe_2O_4 and its variants, represents a promising future direction for creating materials with enhanced properties for various energy-related applications [47, 48].

VIII. FUTURE PERSPECTIVES AND RESEARCH DIRECTIONS

Doping and Surface Modification for Enhanced Performance

A major trend in current research is the strategic modification of NiFe_2O_4 nanoparticles to improve their intrinsic properties and expand their application range. Doping the spinel structure with other elements, such as copper (Cu) or aluminum (Al), has been shown to significantly enhance the material's photocatalytic degradation efficiency by increasing the number of active sites and suppressing the recombination of electron-hole pairs. For instance, a Cu-doped sample demonstrated a 99.85% degradation rate for Rhodamine B dye. This approach reveals that material modification is not merely about adding a new component; it involves deliberately altering the fundamental properties to achieve a desired function. A noteworthy example is the substitution of iron with nickel ions in the ferrite core, which can lead to a lower saturation magnetization but a higher signal in magnetic particle imaging, a result of shorter relaxation times. This observation underscores a critical trade-off in material design: optimizing a material for one application may require compromising its performance in another. This suggests a compelling direction for future research in the development of multi-doped or core-shell structures to achieve a balance of properties for multifunctional applications. Additionally, the use of organic surfactants like polyethylene glycol (PEG) and natural plant extracts points toward a growing trend in surface engineering to enhance particle stability and biocompatibility [47].

Scalability and Economic Viability of Sonochemical Synthesis

While many advanced synthesis methods remain confined to laboratory-scale production, the sonochemical method offers a viable path toward industrial scalability. Its inherent advantages, such as energy efficiency and cost-effectiveness, make it an attractive option for large-scale manufacturing. A techno-economic analysis has already indicated that the production of NiFe_2O_4 via sonochemical synthesis can be a profitable venture, with a projected payback period of just three years under ideal conditions. This economic feasibility is a crucial finding, as it positions the sonochemical method as a practical and sustainable pathway for the future of nanoparticle manufacturing, addressing a significant limitation of many other complex synthesis techniques [49].

Integration into Multifunctional Nanocomposites

The high surface area, reactivity, and magnetic properties of sonochemically synthesized NiFe_2O_4 nanoparticles make them excellent building blocks for the creation of advanced, multifunctional nanocomposites. Research is already exploring the use of these ferrites as components in hybrid systems with materials like activated carbon for applications in environmental remediation. This trend toward material integration allows for the design of systems that can overcome the limitations of single-component materials. For example, a nanocomposite could combine the magnetic separability of NiFe_2O_4 with the high adsorption capacity of another material, enabling highly efficient and recyclable

systems for a wide array of applications. This approach leverages the best attributes of multiple materials to create novel, high-performance solutions [50, 51].

IX. CONCLUSION

The ultrasonic-assisted sonochemical method represents an efficient, green, and cost-effective pathway for the synthesis of NiFe₂O₄ nanoparticles. The mechanism, driven by acoustic cavitation, creates unique localized "hot spots" with extreme temperatures and pressures, which accelerate the formation of highly crystalline and uniformly dispersed particles. The ability to precisely control synthesis parameters such as sonication time, power, pH, and calcination temperature provides a powerful tool for tailoring the nanoparticles' size, morphology, and surface properties. This fine-tuning is crucial for achieving specific magnetic behaviors, such as the transition to a superparamagnetic state, which is a critical characteristic for a number of applications. Looking forward, the economic feasibility of this method and its demonstrated utility in environmental remediation, high-frequency electronics, and biomedical fields like MRI and MPI position it as a promising route for large-scale production. Continued research on doping and multifunctional composites will further expand the potential of these materials.

REFERENCES

- [1] D.-H. Chen, X.-R. He, *Materials research bulletin*, 36 (2001) 1369-1377.
- [2] K. Maaz, S. Karim, A. Mumtaz, S. Hasanain, J. Liu, J. Duan, *Journal of Magnetism and Magnetic Materials*, 321 (2009) 1838-1842.
- [3] N. Gupta, P. Jain, R. Rana, S. Shrivastava, *Materials Today: Proceedings*, 4 (2017) 342-349.
- [4] P. Sivakumar, R. Ramesh, A. Ramanand, S. Ponnusamy, C. Muthamizhchelvan, *Materials Research Bulletin*, 46 (2011) 2208-2211.
- [5] S. Son, M. Taheri, E. Carpenter, V. Harris, M. McHenry, *Journal of Applied Physics*, 91 (2002) 7589-7591.
- [6] B.P. Jacob, A. Kumar, R. Pant, S. Singh, E. Mohammed, *Bulletin of Materials Science*, 34 (2011) 1345-1350.
- [7] S. Sagadevan, Z.Z. Chowdhury, R.F. Rafique, *Materials Research*, 21 (2018) e20160533.
- [8] A.A. Ati, Z. Othaman, A. Samavati, *Journal of Molecular Structure*, 1052 (2013) 177-182.
- [9] J. Wang, F. Ren, R. Yi, A. Yan, G. Qiu, X. Liu, *Journal of Alloys and Compounds*, 479 (2009) 791-796.
- [10] M. Ahamed, M.J. Akhtar, M.A. Siddiqui, J. Ahmad, J. Musarrat, A.A. Al-Khedhairi, M.S. AlSalhi, S.A. Alrokayan, *Toxicology*, 283 (2011) 101-108.
- [11] D.R.A. El-Hafiz, M.A. Ebiad, A.A.-E. Sakr, *Journal of Inorganic and Organometallic Polymers and Materials*, 31 (2021) 292-302.
- [12] Z. Yuan, Z.-h. Chen, D. Chen, Z.-t. Kang, *Ultrasonics sonochemistry*, 22 (2015) 188-197.
- [13] M.S. Amulya, H. Nagaswarupa, M.A. Kumar, C. Ravikumar, S. Prashantha, K. Kusuma, *Applied Surface Science Advances*, 1 (2020) 100023.
- [14] A.M. Ilosvai, D. Dojcsak, C. Váradi, M. Nagy, F. Kristály, B. Fiser, B. Viskolcz, L. Vanyorek, *International journal of molecular sciences*, 23 (2022) 5081.
- [15] P.B. Kharat, S. More, S.B. Somvanshi, K. Jadhav, *Journal of Materials Science: Materials in Electronics*, 30 (2019) 6564-6574.
- [16] M.S. Amulya, H. Nagaswarupa, M.A. Kumar, C. Ravikumar, K. Kusuma, *Applied Surface Science Advances*, 2 (2020) 100038.
- [17] A.A. Ádám, M. Szabados, G. Varga, Á. Papp, K. Musza, Z. Kónya, Á. Kukovecz, P. Sipos, I. Pálinkó, *Nanomaterials*, 10 (2020) 632.
- [18] D. Chen, H.-y. Liu, *Materials Letters*, 72 (2012) 95-97.
- [19] Y. Slimani, E. Hannachi, *Synthesis of ferrite nanoparticles using sonochemical methods, Ferrite Nanostructured Magnetic Materials, Elsevier2023*, pp. 121-147.
- [20] F. Mehrabi, E.A. Dil, *Ultrasonics sonochemistry*, 37 (2017) 37-46.
- [21] Y. Slimani, M. Almessiere, A.D. Korkmaz, A. Baykal, A. Manikandan, H. Gungunes, M. Toprak, *Applied Physics A*, 128 (2022) 593.

- [22] S. Surinwong, A. Rujiwatra, *Particuology*, 11 (2013) 588-593.
- [23] Y. Peng, C. Xia, M. Cui, Z. Yao, X. Yi, *Ultrasonics Sonochemistry*, 71 (2021) 105369.
- [24] M. Abbas, B.P. Rao, C. Kim, *Materials Chemistry and Physics*, 147 (2014) 443-451.
- [25] M.W. Mushtaq, M. Shahbaz, R. Naeem, S. Bashir, S. Sharif, K. Ali, N.A. Dogar, *RSC advances*, 14 (2024) 20230-20239.
- [26] A. Said, A. Abu-Sehly, A. Mahmoud, H. Ahmed, M. Goda, *Journal of Materials Science: Materials in Electronics*, 33 (2022) 16805-16817.
- [27] A.R. Abbasian, Z. Lorfasaeei, M. Shayesteh, M.S. Afarani, *Journal of the Australian Ceramic Society*, 56 (2020) 1119-1126.
- [28] I. Bameri, J. Saffari, S. Baniyaghoob, M.-S. Ekrami-Kakhki, *Colloid and Interface Science Communications*, 48 (2022) 100610.
- [29] M. Kristl, B. Dojer, S. Gyergyek, J. Kristl, *Heliyon*, 3 (2017).
- [30] M. Hosseini, H. Rezaei Ashtiani, D. Ghanbari, *Journal of Nanostructures*, 12 (2022) 588-597.
- [31] H. Harzali, F. Saida, A. Marzouki, A. Megriche, F. Baillon, F. Espitalier, A. Mgaidi, *Journal of Magnetism and Magnetic Materials*, 419 (2016) 50-56.
- [32] A.D. Korkmaz, *Materials Science and Engineering: B*, 295 (2023) 116598.
- [33] S.M. Abdulkareem, R.M. Alsaffar, G.H.A. Razzaq, J.H. Mohammed, T.M. Awad, M.A. Alheety, L.A. Mohammed, A.H. Mageed, E.M. Ali, A.H. Dalaf, *Journal of Sol-Gel Science and Technology*, 111 (2024) 979-988.
- [34] P.E. Meskin, V.K. Ivanov, A.E. Barantchikov, B.R. Churagulov, Y.D. Tretyakov, *Ultrasonics sonochemistry*, 13 (2006) 47-53.
- [35] Z. Zhang, G. Yao, X. Zhang, J. Ma, H. Lin, *Ceramics International*, 41 (2015) 4523-4530.
- [36] T. Dippong, O. Cadar, F. Goga, D. Toloman, E.A. Levei, *International Journal of Molecular Sciences*, 23 (2022) 14167.
- [37] M.S. Amulya, H. Nagaswarupa, M.A. Kumar, C. Ravikumar, K. Kusuma, *Journal of Physics and Chemistry of Solids*, 148 (2021) 109661.
- [38] F. Kiani, H. Naeimi, *Ultrasonics Sonochemistry*, 48 (2018) 267-274.
- [39] I. Hasan, A. Bassi, K.H. Alharbi, I.I. BinSharfan, R.A. Khan, A. Alslame, *Coatings*, 10 (2020) 1200.
- [40] L. Frolova, O. Kushnerov, A. Derimova, 2017 XXIInd International Seminar/Workshop on Direct and Inverse Problems of Electromagnetic and Acoustic Wave Theory (DIPED), IEEE2017, pp. 84-87.
- [41] E.K. Nyutu, W.C. Conner, S.M. Auerbach, C.-H. Chen, S.L. Suib, *The Journal of Physical Chemistry C*, 112 (2008) 1407-1414.
- [42] F.I. Haq, M.A.N. Zein, R. Gabriella, S.R. Putri, A.B.D. Nandiyanto, T. Kurniawan, *International Journal of Sustainable Transportation Technology*, 4 (2021) 42-52.
- [43] V. Hajdu, G. Muranszky, A. Prekob, F. Kristaly, B. Fiser, J. Lakatos, B. Viskolcz, L. Vanyorek, *Journal of Materials Research and Technology*, 19 (2022) 3624-3633.
- [44] H. Ahankar, A. Ramazani, K. Ślepokura, T. Lis, V. Kinzhybalov, *Research on Chemical Intermediates*, 45 (2019) 5007-5025.
- [45] N.-D. Jaji, H.L. Lee, M.H. Hussin, H.M. Akil, M.R. Zakaria, M.B.H. Othman, *Nanotechnology reviews*, 9 (2020) 1456-1480.
- [46] M. Bouchenak, K. Boutemak, A. Haddad, B. Boutra, *Environmental Science and Pollution Research*, (2025) 1-15.
- [47] B. Tang, L. Yuan, T. Shi, L. Yu, Y. Zhu, *Journal of Hazardous Materials*, 163 (2009) 1173-1178.
- [48] W. Azouzi, I. Boulahya, J. Robert, A. Essyed, A. Mahmoud, A. Al Shami, D. Ihiawakrim, H. Labrim, M. Benaissa, *Ultrasonics Sonochemistry*, 111 (2024) 107108.
- [49] K.O. Abdulwahab, M.M. Khan, J.R. Jennings, *Critical Reviews in Solid State and Materials Sciences*, 49 (2024) 807-855.
- [50] Z. Li, J. Dong, H. Zhang, Y. Zhang, H. Wang, X. Cui, Z. Wang, *Nanoscale Advances*, 3 (2021) 41-72.
- [51] M.A. Ahmed, A.A. Mohamed, *Iscience*, 27 (2024).